Syntheses, Structures, Thermal and Photoluminescence Properties of Two Zn(II) and Cd(II) Coordination Polymers Constructed from Taurine-derived Schiff Base and 4,4'-Bipyridine Ligands

Wei-Ting Guo, Zhi-Min Miao and Yun-Long Wang

Gout Laboratory, The Affiliated Hospital of Medical College Qingdao University, 16 Jiangsu Road, Qingdao 266003, P. R. China

Reprint requests to Prof. Dr. Yun-Long Wang and Zhi-Min Miao.
E-mail: wangyunlongqd@163.com and miao_zhimin@126.com

Z. Naturforsch. **2012**, *67b*, 774 – 782 / DOI: 10.5560/ZNB.2012-0170
Received June 15, 2012

Two chain-like coordination polymers, namely, $\{[Zn(saes)(4,4'\text{-bipy})(H_2O)]\cdot H_2O\}_n$ (**1**) and $\{[Cd(Hsaes)_2(4,4'\text{-bipy})(H_2O)_2]\cdot 2H_2O\}_n$ (**2**), where H_2saes = 2-(2-hydroxybenzylideneamino)ethanesulfonic acid and 4,4'-bipy = 4,4'-bipyridine, have been synthesized and characterized by single-crystal X-ray diffraction, IR spectroscopy, elemental, thermogravimetric and photoluminescence analysis. X-Ray diffraction analyses indicate that **1** and **2** display octahedral metal centers with N_3O_3 and N_2O_4 donor sets, respectively. The Schiff base serves as a common *N*,*O*,*O*'-tridentate ligand in **1**, and as a unique *O*-monodentate ligand in **2**. In the crystal, both **1** and **2** form a 3D supramolecular architecture by O–H···O, C–H···O interactions or $\pi\cdots\pi$ stacking. The thermal and solid-state photoluminescence properties of both complexes have been investigated.

Key words: Coordination Polymer, Luminescence Properties, 4,4'-Bipyridine, Taurine Schiff Base, Crystal Structure

Introduction

In the past decades, the research on Schiff bases has gained considerable interest due to a diverse range of applications, such as liquid crystals [1], heterogeneous catalysts [2] and organic synthesis [3, 4]. Various Schiff base ligands have been studied in coordination chemistry [5 – 19], aiming at a better understanding of chemical and structural factors in physics, biology and chemistry [20 – 23]. Furthermore, transition metal complexes of Schiff bases containing both sulfur and amino acid functionality have received considerable attention due to their anticancer, antibacterial and antiviral activities [23]. 2-Aminoethanesulfonic acid, known as taurine, a non-protein amino acid containing sulfur which is indispensable to human beings and animals, plays an important part in physiological functions.

The coordination modes of the taurine Schiff base have been scarcely studied. Recently, Jiang's and Vittal's groups were interested in tridentate Schiff base ligands, specifically 2-(2-hydroxybenzylideneamino)ethanesulfonic acid, and they found that the Schiff base derived from taurine has manifold coordination modes [16, 23 – 26]. The most common coordination modes are tridentate and bidentate, while monodentate is very rare. Moreover, sulfonate ligands have been much less studied since they are weakly coordinating ligands [3]. In fact, the sulfonate group, as a tetrahedral oxygen-donating building block, may bridge sites of coordination polymer chains to dictate the interchain geometry. Following the above consideration and ongoing work in this field, we present the synthesis and structures of the compounds $\{[Zn(saes)(4,4'\text{-bipy})(H_2O)]\cdot H_2O\}_n$ (**1**) and $\{[Cd(Hsaes)_2(4,4'\text{-bipy})(H_2O)_2]\cdot 2H_2O\}_n$ (**2**) (Scheme 1), which have been structurally characterized by single-crystal X-ray diffraction, and their thermal stability and luminescence properties. The X-ray crystal structure analysis of **1** has demonstrated that the taurine Schiff base ligand acts as a tridentate moiety, coordinating through the phenolato oxygen,

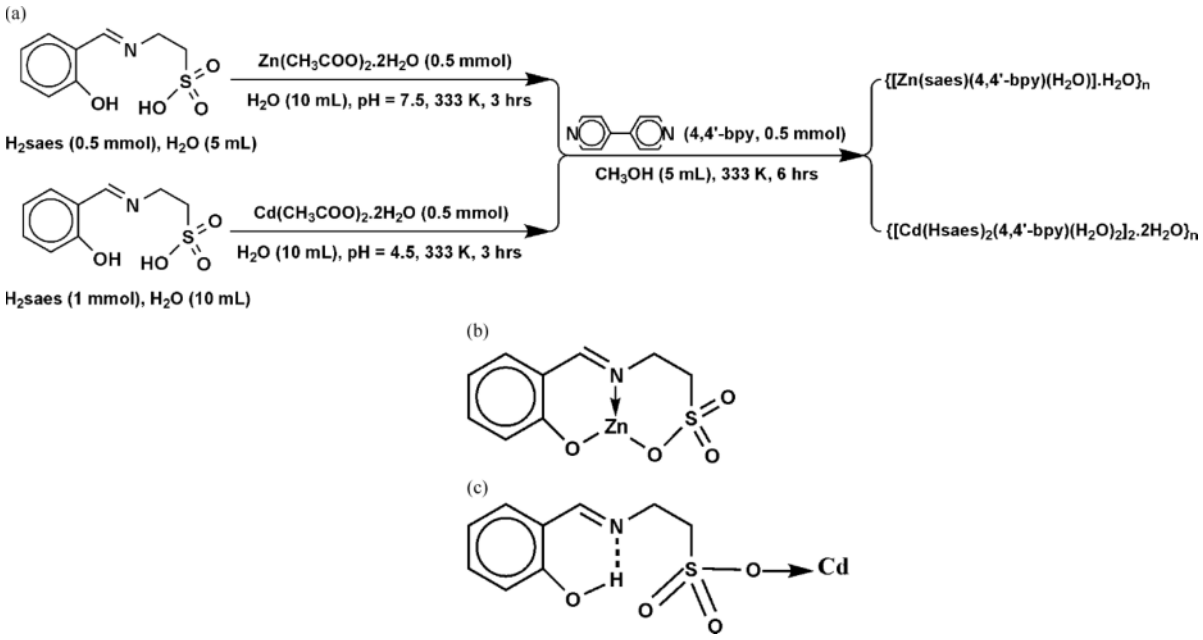

Scheme 1. (a) The synthesis for **1** and **2**; (b) view of the coordination mode of the $saes^{2-}$ ligand in **1**; (c) view of the coordination mode of the $Hsaes^{-}$ ligand in **2**.

imine nitrogen, and sulfonate oxygen atoms. However, a unique coordination mode of the Schiff base ligand appeared in **2**, where it acts in a monodentate fashion *via* one of the sulfonate oxygen atoms.

Results and Discussion

*The crystal and molecular structure of {[Zn(saes)(4,4'-bpy)(H$_2$O)]·H$_2$O}$_n$ (**1**)*

The single-crystal X-ray diffraction analysis revealed that **1** is a 1D coordination polymer, whose asymmetric unit is comprised of one Zn^{2+}, one doubly deprotonated tridentate chelating H_2saes, *i.e.* $saes^{2-}$, one 4,4'-bipy, one H_2O ligand and an interstitial solvate water molecule (Fig. 1a). The Zn(II) ion is hexacoordinated with O1, O2 and N1 atoms from $saes^{2-}$, N2 and N3A atoms from two different μ_2-bridging 4,4'-bipy ligands, and O1W from a water molecule, displaying a distorted octahedral geometry (Fig. 1a and Table 1). The equatorial plane of **1** is defined by the three donor atoms [O(1), O(2), N(1)] of the $saes^{2-}$ ligand, the other atom belonging to coordinated water [O(1w)] at a mean distance close to 2.1 Å. The two N atoms [N(2), N(3A)] from two different μ_2-bridging 4, 4'-bipy units are situated at the axial sites with a bond angle of 170.76(9)°. Zn1 resides out of the O_3N equatorial plane towards N2 by 0.018 Å. The Zn–O bond lengths range from 2.0312(19) to 2.152(2) Å, and those of Zn–N bonds are 2.125(2) to 2.227(2) Å. The sum of the bond angles O(1W)–Zn1–O2 (87.85(9)°), O1–Zn1–N1 (88.32(8)°), N1–Zn1–

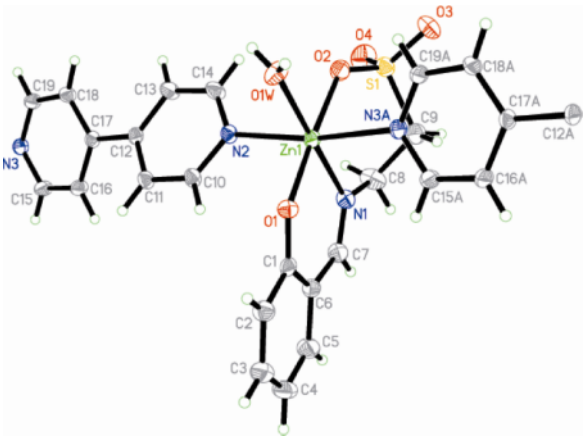

Fig. 1a (color online). The coordination environment of the Zn(II) ion in **1** drawn at 30 % probability displacement ellipsoids. (Symmetry code: A: $1+x$, y, $1+z$).

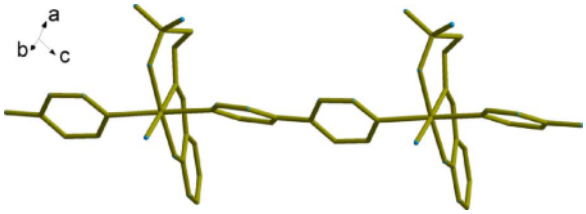

Fig. 1b (color online). A segment of the chain structure of **1**. (C atoms have been drawn as wires and H atoms omitted for clarity).

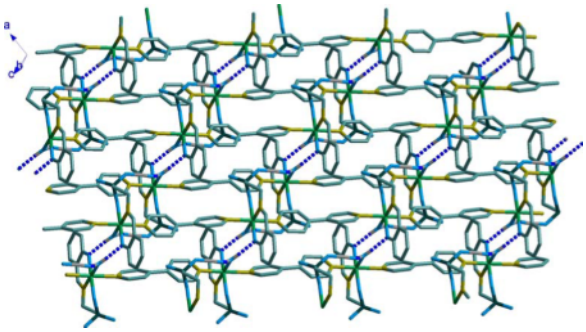

Fig. 1c (color online). Plot of the 2D hydrogen bonding (dashed lines) structure of **1**. (H atoms have been omitted, except those involved in hydrogen bonds).

O2 (90.40(9)°), and O1–Zn1–O(1W) (93.45(8)°) is 360.02°, showing that O1, O2, O(1w) and N1 atoms are well coplanar.

The Schiff base ligand ($saes^{2-}$) is coordinated meridionally to Zn *via* its imine N and deprotonated phenolate and sulfonate oxygen atoms, forming two edge-sharing six-membered chelate rings (Scheme 1). The ring containing Zn1–O1–C1–C6–C7–N1 is planar (mean r. m. s. deviation of 0.0446 Å), and the ring containing the sulfonate group has an envelop conformation with C9 maximally deviating from the Zn1–N1–C8–C9–S1–O2 plane by 0.50 Å. The O–C1–C angles are markedly unsymmetrical (119.9(3) and 123.2(3)°) as a result of the chelating coordination. Furthermore, the substituents at the N1–C7 bond form an eclipsed conformation, as noted from the C6–C7–N1–C8 torsion angle of 179.7(3)°. The C7–N1 bond length of 1.282(4) Å is indicative of a C=N double bond, as compared to C8–N1 with 1.475(4) Å, which is in the range of C–N single bonds. The S–O(Zn) bond (1.464(2) Å) is marginally longer than the uncoordinated S–O bonds (1.437(3) and 1.456(3) Å).

The building blocks [Zn(saes)(H_2O)] are tied together with pairs of μ_2-bridging 4,4'-bipy ligands, leading to an infinite chain structure along the [001] direction (Fig. 1b). A Zn···Zn separation of 11.47 (2) Å is found between the neighboring [Zn(saes)(H_2O)] repeating units.

The chains interact with each other into reverse alternate arrangements shown in Fig. 1c. The neighboring 1D coordination polymers are connected by pairs of intermolecular O–H···O hydrogen bonds of the coordinating phenolate, the uncoordinated sulfonate and coordinating water O atoms (O1, O4, O1W), resulting in a layer structure parallel to the (110) plane (Fig. 1c and Table 2). The shortest Zn···Zn distance of 5.10(2) Å is observed between neighboring chains. In addition, the neighboring layers are linked by non-classical intermolecular C–H···O hydrogen bonds of phenolate and sulfonate oxygen atoms (O1, O2 and O3) with C···O distances in the range 3.054(4) to 3.318(4) Å. However, their contribution to the overall lattice energy must be very small. Thus a supramolecular 3-D network fragment is formed by O–H···O and C–H···O interactions and stabilizing the coordination polymer.

*The crystal and molecular structure of {[Cd(Hsaes)$_2$(4,4'-bpy)(H_2O)$_2$]·2H_2O}$_n$ (**2**)*

The single-crystal X-ray diffraction analysis has revealed that **2** is also a 1D coordination polymer, whose asymmetric unit is comprised of one Cd^{2+}, one 4,4'-bipy, two $Hsaes^-$, two H_2O ligands, and two solvate

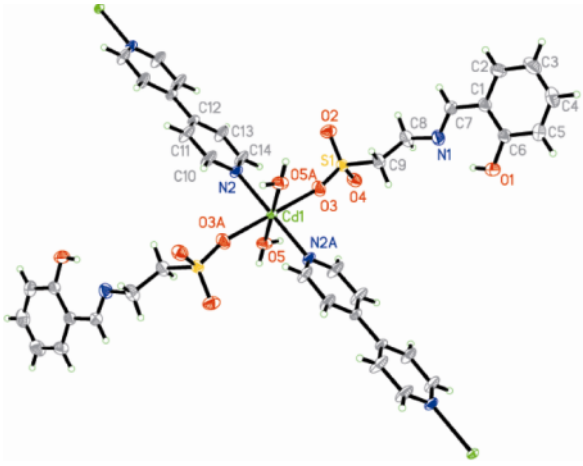

Fig. 2a (color online). The coordination environment of the Cd(II) ion in **2** drawn with 30% probability displacement ellipsoids. (Symmetry code: A: $1-x$, $1-y$, $2-z$).

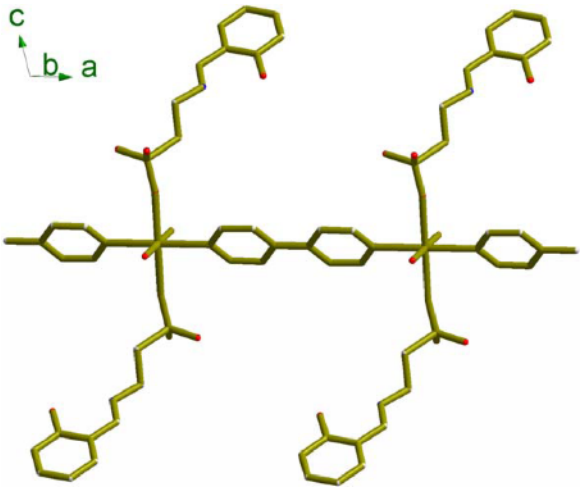

Fig. 2b (color online). A segment of the chain structure of **2** along the crystallographic *a* axis (C atoms have been drawn as wires and H atoms omitted for clarity).

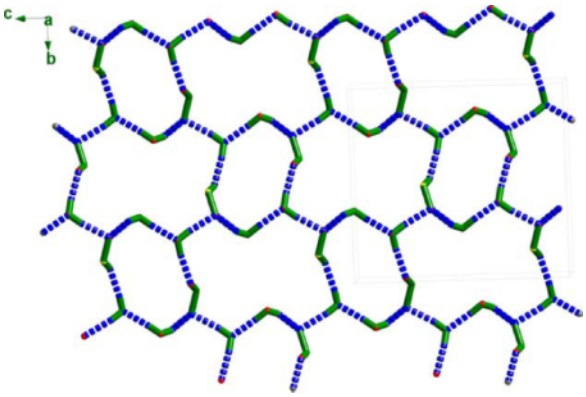

Fig. 2c (color online). Plot of the 2-D hydrogen bonding (dashed lines) network in **2**. (H atoms have been omitted, except those involved in hydrogen bonds).

water molecules (Fig. 2a). Each Cd atom is octahedrally coordinated and located at a center of symmetry (Fig. 2a and Table 1). The four O atoms from two singly deprotonated tridentate H_2saes (Hsaes$^-$) and two H_2O ligands define the equatorial plane with the Cd center located in the plane, and two N atoms of two different 4,4'-bipy ligands in the axial positions with an N2–Cd1–N2A angle of 180°. The length of the Cd–N bond is 2.2793(15) Å; the lengths of Cd–O bonds are 2.3099(15) and 2.3248(14) Å.

The Schiff base ligand Hsaes$^-$ is monodentately coordinated to Cd *via* its deprotonated sulfonate oxygen atom. To the best of our knowledge, monoden-

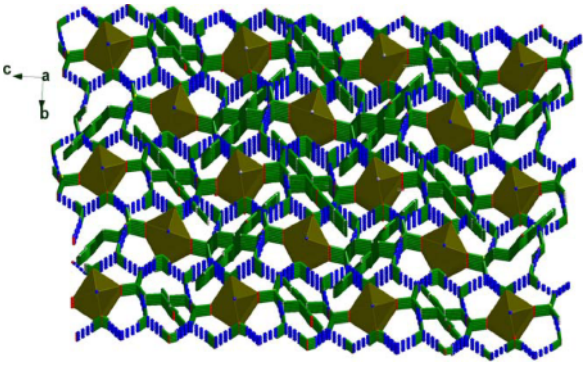

Fig. 2d (color online). View of 3-D network for **2**, showing O–H···O hydrogen bonding as dashed lines. (H atoms have been omitted, except those involved in hydrogen bonds).

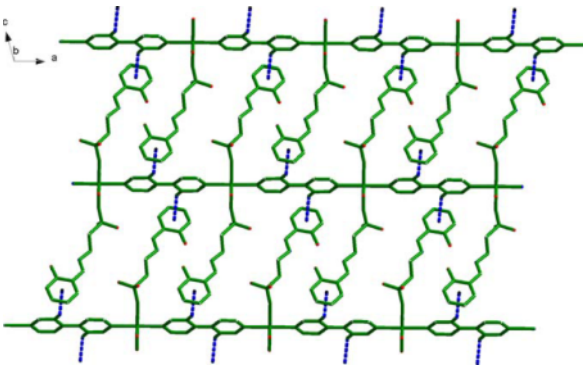

Fig. 2e (color online). The 2D packing of the complex for **2**, showing C–H···π stackings as dashed lines. (H atoms have been omitted, except those involved in C–H···π stacking).

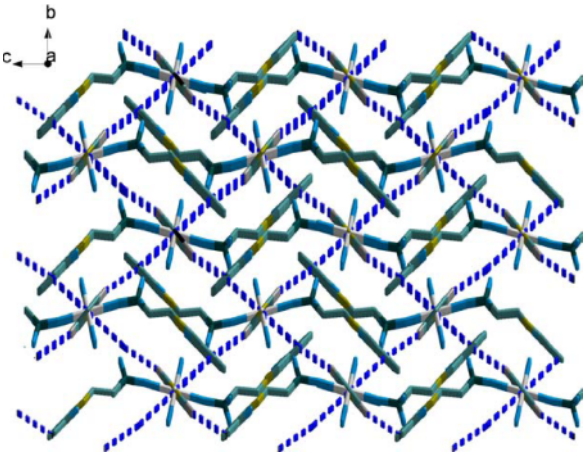

Fig. 2f (color online). View of 3-D network for **2**, showing C–H···π and π···π stackings as dashed lines. (H atoms have been omitted, except those involved in C–H···π stacking).

Table 1. Selected bond lengths (Å) and angles (deg) for **1** and **2** with estimated standard deviations in parentheses.

Compound **1**[a]			
Zn1–O1	2.0312(19)	Zn1–O1W	2.086(2)
Zn1–N1	2.125(2)	Zn1–O2	2.152(2)
Zn1–N2	2.194(2)	Zn1–N3^{i}	2.227(2)
S1–O3	1.437(3)	S1–O4	1.456(3)
S1–O2	1.464(2)	S1–C9	1.775(3)
O1–Zn1–O1W	93.45(8)	O1–Zn1–N1	88.32(8)
O1W–Zn1–N1	178.16(9)	O1–Zn1–O2	177.22(8)
O1W–Zn1–O2	87.85(9)	N1–Zn1–O2	90.40(9)
O1–Zn1–N2	94.67(8)	O1W–Zn1–N2	85.23(8)
N1–Zn1–N2	94.13(9)	O2–Zn1–N2	87.89(9)
O1–Zn1–N3^{i}	89.26(8)	O1W–Zn1–N3^{i}	86.19(8)
N1–Zn1–N3^{i}	94.34(9)	O2–Zn1–N3^{i}	88.36(9)
N2–Zn1–N3^{i}	170.76(9)	O3–S1–O4	113.39(17)
O3–S1–O2	112.07(16)	O4–S1–O2	112.21(15)

[a] Symmetry code: ^{i} $x+1, y, z+1$.

Compound **2**[b]			
Cd1–N2	2.2793(15)	S1–O2	1.4423(15)
Cd1–O5	2.3091(15)	S1–O3	1.4518(14)
Cd1–O3	2.3247(13)	S1–O4	1.4568(15)
S1–C9	1.777(2)	N1–C7	1.267(3)
N2–Cd1–N2^{i}	180	O5–Cd1–O5^{i}	180
N2–Cd1–O5^{i}	90.31(5)	N2–Cd1–O3	90.41(6)
N2^{i}–Cd1–O5^{i}	89.69(5)	N2–Cd1–O3^{i}	89.59(6)
N2–Cd1–O5	89.69(5)	O5–Cd1–O3^{i}	94.52(6)
N2–Cd1–O5^{i}	90.31(5)	O5–Cd1–O3	85.48(6)
N2–Cd1–O3^{i}	89.59(6)	N2^{i}–Cd1–O3^{i}	90.41(6)
O5^{i}–Cd1–O3^{i}	85.48(6)	O5–Cd1–O3^{i}	94.52(6)
O3–Cd1–O3^{i}	180.0	O2–S1–O3	113.81(10)
O2–S1–O4	111.94(9)	O3–S1–O4	111.26(9)
O2–S1–C9	107.82(10)	O3–S1–C9	104.58(10)
O4–S1–C9	106.85(10)	S1–O3–Cd1	165.77(11)

[b] Symmetry code: ^{i} $-x+1, -y+1, -z+2$.

tate coordination of the tridentate taurine Schiff base is rare. The initial subunits $[Cd(Hsaes)(H_2O)]_2$ are tied together with pairs of μ_2-bridging 4,4'-bipy ligands, leading to an infinite chain structure along the [110] direction (Fig. 2b). A Cd···Cd separation of 11.65(2) Å is observed for adjacent $[Cd(Hsaes)(H_2O)]_2$ units.

In the crystal structure, an intramolecular O–H···N hydrogen bond produces an S_6-ring motif through the uncoordinated Schiff base N atom (acceptor) and the unprotonated phenolic hydroxyl group (donor). By contrast, the water molecules and sulfonate groups participate in intermolecular O–H···O hydrogen bonds (Table 2), which link the chains in reversely alternating parallel arrangements, defining a 3D hydrogen-bonded network and supporting the supramolecular architecture (Figs. 2c and 2d). Furthermore, two significant interchain π stacking interactions are observed. C–H··π interactions interlink adjacent chains with H(11)···centroid distances of 2.97 Å between flanking phenyl rings, forming an interdigitated packing motif. The phenyl rings of $Hsaes^{-}$ and pyridyl rings of the 4,4'-bpy ligands of neighboring chains are interdigital to each other, and there are face-to-face π···π-stacking interactions with a centroid-to-centroid distance of *ca.* 3.87 Å. Thus, these layers are extended into an interwoven 3D supramolecular architecture through C–H··π and π···π interactions, which further support the hydrogen-bonded (O–H···O) network (Figs. 2e and 2f).

Clearly, the structural differences between **1** and **2** are mainly due to the taurine Schiff base coordination modes at different metals, and the different deprotonation state of the taurine Schiff base. In compound **1**, the coordination sphere at the Zn(II) center is a distorted octahedral geometry, but the coordination environment of the Cd(II) center has an ideal octahedron in **2**. In addition, a 3D supramolecular architecture is formed by O–H···O and C–H···O hydrogen bonds interactions in

Table 2. Hydrogen bonding geometries (Å, deg) for **1** and **2** with estimated standard deviations in parentheses.

D–H···A	*d*(D–H)	*d*(H···A)	*d*(D···A)	∠(D–H···A)
Compound **1**[a]				
O2W–H2B···O(4)[ii]	0.86(1)	1.84(2)	2.693(4)	169(6)
O1W–H1B···O1[iii]	0.82(1)	1.84(1)	2.646(3)	169(3)
O1W–H1C···O(2W)[iii]	0.82(1)	1.97(2)	2.752(4)	159(3)
[a] Symmetry codes: [ii] $x, y, z+1$; [iii] $-x+1, -y+2, -z+1$.				
Compound **2**[b]				
O1–H1···N1	0.828(10)	1.843(19)	2.596(2)	151(3)
O5–H1W···O4[ii]	0.811(9)	2.049(12)	2.838(2)	164(2)
O5–H2W···O6	0.822(9)	1.896(11)	2.710(3)	170(3)
O6–H3W···O2[iii]	0.86	1.92	2.770(2)	172.8
O6–H4W···O4	0.86	1.95	2.807(2)	172.5
O6–H4W···O3	0.86	2.59	3.170(2)	125.5
[b] Symmetry codes: [ii] $x, -y+3/2, z+1/2$; [iii] $-x+1, y+1/2, -z+3/2$.				

1, but through O–H···O as well as C–H···π and $\pi\cdots\pi$ stacking in **2**.

*Thermogravimetric analyses of **1** and **2***

In order to explore the thermal stability of these materials, TG studies have been performed in nitrogen at a heating rate of 10 °C min^{-1} between 20 and 900 °C. For compound**1**, a weight loss of 7.4 % was observed below 115 °C, which is attributed to the release of the coordinating and free water molecules (calcd. 7.5 %). Then the decomposition of the framework occurred at about 230 °C (Fig. 3) corresponding to the loss of 4,4'-bipyridine ligands (obsd: 35.4; calcd: 35.5 %) in the temperature range 230 – 380 °C. Therefore, it can be assumed that during this thermal reaction Zn(saes) fragments are formed, which decompose in the temperature range 390 – 550 °C. Above that decomposition almost no weight loss is observed up to 550 °C, the final residue probably being ZnO (found: 26.4; calcd. 26.5 %). In the case of **2**, there was a weight loss of 9.0 % below 142 °C, which is attributed to the release of coordinating and free water molecules (calcd. 9.1 %), and then the decomposition of the framework occurred at about 240 °C. The second weight loss takes place at 350 °C and corresponds to the loss of Hsaes$^-$ and 4,4'-bipyridine ligands (obsd: 71.7; calcd: 71.6 %) in the temperature range 350 – 550 °C. Above 700 °C the final residue was probably CdO but this was not ascertained by powder diffraction (found: 26.2; calcd. 26.3 %).

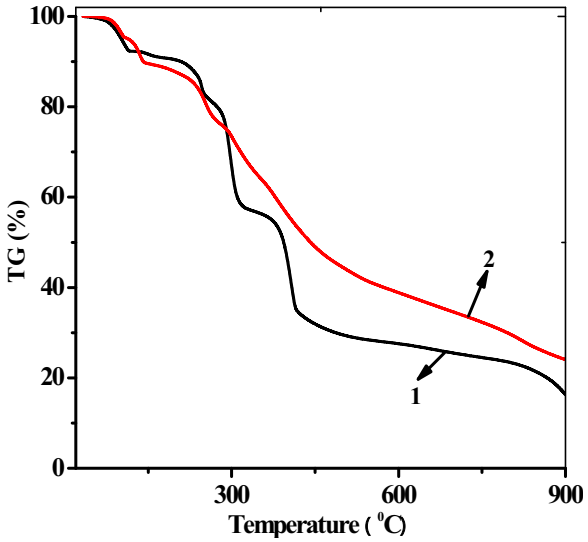

Fig. 3 (color online). TG analyses of **1** and **2**.

*Fluorescence properties of **1** and **2***

The d^{10} metal coordination polymers are widely investigated nowadays for their photoluminescence properties and potential applications as fluorescence-emitting crystalline multifunctional materials, due to their high thermal stability and the possibility to affect the emission wavelength of the modified organic ligand *via* metal coordination [27 – 29]. Therefore, solid-state emission spectra of the Zn(II) and Cd(II) coordination polymers **1** and **2** have been investigated at r. t. As depicted in Fig. 4, compound **1** exhibits an intense emission with a maximum at 490 nm upon photoexcitation at 360 nm. The intense emission of the coordination polymer **2** was observed in the range of 350 – 450 nm. To understand the nature of the emission bands, the free ligand was investigated in the solid state at room temperature. An intense emission peak at

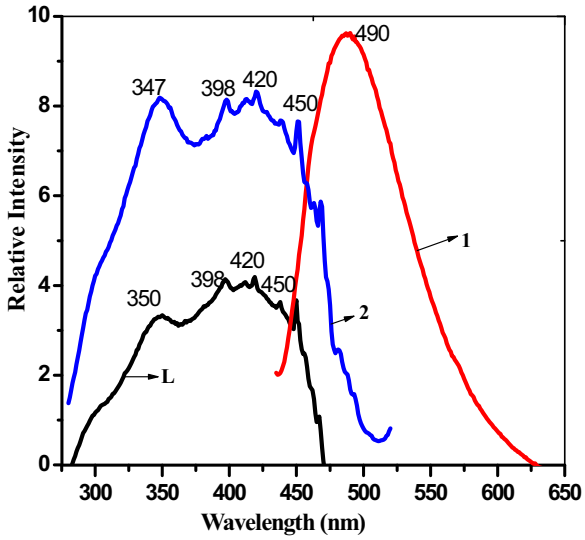

Fig. 4 (color online). Solid-state photoluminescence spectra of **1** and **2** at room temperature.

420 nm upon excitation at 360 nm is observed in the range of 350 – 450 nm, which is attributable to π-π^* transitions. Compared with the free ligand, the band of **1** has a different shape and position representing a strong blue emission at 490 nm. The red-shift can be attributed to coordination of the ligands to Zn centers, which results in an increase of the delocalization of π electrons and reduces the energy gap between the π^* and π molecular orbitals of the ligand [30, 31]. The enhanced emission intensity of **2** comes from two parts. One is the coordination effect [32], and the other is hydrogen bonding [33]. Compared with the free ligand, **2** has a similar band shape and position with high intensity. The emission of **2** is neither a metal-to-ligand charge transfer (MLCT) nor a ligand-to-metal charge transfer (LMCT), because there is no blue or red-shift observed, but may be assigned to intraligand (π-π^*) emission, namely, ligand-to-ligand charge transfer (LLCT). The fluorescence enhancement for **2** is mainly due to hydrogen bonding [34].

Conclusions

We have synthesized two new 1D Zn(II) and Cd(II) coordination polymers with a Schiff base ligand containing a taurine moiety. Both complexes exhibit chains of their building blocks to construct 2D and 3D supramolecular frameworks by O–H···O hydrogen bonds or π-π stacking. The H_2saes ligand coordinates to the metal cations in different fashions: $saes^{2-}$ in **1** can be described as a *O*',*N*,*O*-tridentate chelating ligand, while $Hsaes^-$ in **2** is in a rare *O*-monodentate mode.

Experimental

Materials and physical methods

All starting chemicals were commercially available and used as received without further purification. Elemental analyses (C, H, N) were performed on a Perkin-Elmer 2400II elemental analyzer. FT-IR spectra were recorded from KBr pellets in the range of 4000 – 450 cm^{-1} on a Bio-Rad FTS-7 spectrometer. Thermogravimetric analyses (TGA) were performed under nitrogen with a heating rate of 10 °C min^{-1} using a Netzsch STA 449C thermogravimetric analyzer. Fluorescence spectra were obtained from a 970CRT spectrofluorophotometer.

*Synthesis of {[Zn(saes)(4,4'-bpy)(H_2O)]·H_2O}$_n$ (**1**)*

H_2Saes (0.115 g, 0.5 mmol) dissolved in distilled water (5 mL) was added dropwise to a stirred solution of $Zn(CH_3COO)_2{\cdot}2H_2O$ (0.11 g, 0.5 mmol) in water (10 mL). For this solution, the pH value was adjusted to 7.5 with NaOH (1.0 M), and the resulting mixture was stirred at 333 K for 3 h. Then 5 mL of a methanol solution of 4,4'-bipyridine (0.078 g, 0.5 mmol) was added slowly, and the reaction continued for 6 h. The mixture was cooled to r. t. and filtered. The filtrate was allowed to slowly concentrate by evaporation at r. t. Two weeks later, colorless block-shaped crystals suitable for X-ray structure analysis were obtained in a yield of 10 % (based on Zn). – $C_{19}H_{21}ZnN_3O_6S$ (484.85): calcd. C 47.02, H 4.33, N 8.66; found C 47.07, H 4.30, N 8.64. – IR (KBr): $\nu = 3438$ (m), 1624 (s), 1602 (m), 1539 (m), 1468 (m), 1446 (m), 1411 (m), 1316 (w), 1249 (m), 1214 (m), 1175 (s), 1150 (m), 1069 (w), 1040 (s), 817 (w), 755 (m), 746 (m), 629 (m), 514 (w) cm^{-1}.

*Synthesis of {[Cd(Hsaes)$_2$(4,4'-bpy)(H_2O)$_2$]·$2H_2O$}$_n$ (**2**)*

H_2Saes (0.229 g, 1 mmol) dissolved in distilled water (10 mL) was added dropwise to a stirred solution of $Cd(CH_3COO)_2{\cdot}2H_2O$ (0.5 mmol, 0.133 g) in water (10 mL). This solution had a pH value of 4.5 and was stirred at 333 K for 3 h. Then 5 mL of a methanol solution of 4,4'-bipyridine (0.078 g, 0.5 mmol) was added slowly, and the reaction continued for 6 h. The mixture was cooled to r. t. and filtered. The filtrate was allowed to slowly concentrate by evaporation at r. t. Two weeks later, colorless block-shaped crystals suitable for X-ray structure analysis were obtained in a yield of 20 % (based on Cd). – $C_{28}H_{36}CdN_4O_{12}S_2$ (797.13): calcd. C 42.15, H 4.52, N 7.03; found C 42.12, H 4.54, N 7.01.

Table 3. Crystal structure data for **1** and **2**.

Compound	**1**	**2**
Formula	$C_{19}H_{21}ZnN_3O_6S$	$C_{28}H_{36}CdN_4O_{12}S_2$
M_r	484.85	797.16
Crystal size, mm^3	0.30 × 0.15 × 0.10	0.33 × 0.20 × 0.15
Crystal system	monoclinic	monoclinic
Space group	$P2_1/c$	$P2_1/c$
a, Å	9.4611(5)	11.6504(8)
b, Å	21.2746(9)	11.4625(8)
c, Å	10.6094(6)	13.1879(9)
β, deg	110.554(2)	105.2630(10)
V, Å^3	1999.53(18)	1699.0(2)
Z	4	2
D_{calcd}, g cm^{-3}	1.61	1.56
μ(MoK_α), cm^{-1}	1.4	0.8
F(000), e	1000.0	816
hkl range	–10→11, –25→22, ±12	–15→14, –11→14, ±17
θ range, deg	2.26 – 25.6	2.54 – 27.49
Refl. measd. / unique / R_{int}	13121 / 3750 / 0.0221	10069 / 3864 / 0.0132
Param. refined	283	220
$R(F)$ / $wR(F^2)$[a,b] (all refl.)	0.0410 / 0.0904	0.0277 / 0.0607
GoF (F^2)[c]	1.022	1.061
$\Delta\rho_{fin}$ (max / min), e Å^{-3}	0.48 / −0.49	0.44 / −0.36

[a] $R = \Sigma||F_o| - |F_c||/\Sigma|F_o|$; [b] $wR2 = [\Sigma w(F_o^2 - F_c^2)^2/\Sigma w(F_o^2)^2]^{1/2}$, $w = [\sigma^2(F_o^2) + (AP)^2 + BP]^{-1}$, where $P = (\mathrm{Max}(F_o^2, 0) + 2F_c^2)/3$; [c] GoF $= [\Sigma w(F_o^2 - F_c^2)^2/(n_{obs} - n_{param})]^{1/2}$.

– IR (KBr): $\nu = 3449$ (s), 1641 (s), 1602 (m), 1578 (m), 1532 (w), 1479 (m), 1414 (m), 1282 (w), 1235 (m), 1201 (s), 1161 (m), 1050 (m), 918 (w), 807(m), 745 (m), 629 (m) cm^{-1}.

X-Ray crystallographic studies

Single-crystal data collections were carried out on a Bruker Smart Apex II CCD diffractometer with graphite-monochromatized MoK_α radiation ($\lambda = 0.71073$ Å) at 296(2) K. The structures were solved with Direct Methods using SHELXS-97 [35], and structure refinements were performed against F^2 using SHELXL-97 [36]. All non-hydrogen atoms were refined with anisotropic displacement parameters. Carbon-bound H atoms were placed in calculated positions ($d_{C-H} = 0.93 - 0.97$ Å) and were included in the refinement in the riding model approximation, with U_{iso}(H) set to 1.2U_{eq}(C). The water and hydroxyl H atoms were located in a difference Fourier map, and were refined with distance restraints. Their temperature factors were tied to those of the parent atoms by a factor of 1.5. Further details of the structure determinations are summarized in Table 3.

CCDC 614217 (**1**) and CCDC 629383 (**2**) contain the supplementary crystallographic data for this paper. These data can be obtained free of charge from The Cambridge Crystallographic Data Centre *via* www.ccdc.cam.ac.uk/data_request/cif.

Acknowledgement

This work was supported by Gout laboratory, the Affiliated Hospital of Qingdao University Medical College.

[1] N. Hoshino, *Coord. Chem. Rev.* **1998**, *174*, 77 – 108.
[2] L. Canali, D. C. Sherrington, *Chem. Soc. Rev.* **1999**, *28*, 85 – 93.
[3] T. Katsuki, *Coord. Chem. Rev.* **1995**, *140*, 189 – 214.
[4] Y. N. Ito, T. Katsuki, *Bull. Chem. Soc. Jpn.* **1999**, *72*, 603 – 619.
[5] W. L. Leong, J. J. Vittal, *Chem. Rev.* **2011**, *111*, 688 – 746.
[6] R. Ganguly, B. Sreenivasulu, J. J. Vittal, *Coord. Chem. Rev.* **2008**, *252*, 1027 – 1050.
[7] P. A. Vigato, S. Tamburini, *Coord. Chem. Rev.* **2004**, *248*, 1717 – 2128.
[8] B. Sreenivasulu, J. J. Vittal, *Inorg. Chim. Acta* **2009**, *362*, 2735 – 2743.
[9] B. Y. Lou, D. Q. Yuan, S. Y. Gao, R. H. Wang, Y. Xu, L. Han, M. C. Hong, *J. Mol. Struct.* **2004**, *707*, 231 – 234.
[10] B. Y. Lou, D. Q. Yuan, R. H. Wang, Y. Xu, B. L. Wu, L. Han, M. C. Hong, *J. Mol. Struct.* **2004**, *689*, 87 – 91.

[11] B. Sreenivasulu, J. J. Vittal, *Angew. Chem. Int. Ed.* **2004**, *43*, 5769 – 5772.
[12] C. T. Yang, M. Vetrichelvan, X. D. Yang, B. Moubaraki, K. S. Murray, J. J. Vittal, *Dalton Trans.* **2004**, 113 – 121.
[13] A. Mukherjee, M. K. Saha, M. Nethaji, A. R. Chakravarty, *Chem. Commun.* **2004**, 716 – 717.
[14] Y. B. Dong, X. Zhao, B. Tang, H. Y. Wang, R. Q. Huang, M. D. Smith, H. C. zur Loye, *Chem. Commun.* **2004**, 220 – 221.
[15] S. Kitagawa, R. Kitaura, S. Noro, *Angew. Chem. Int. Ed.* **2004**, *43*, 2334 – 2375.
[16] B. Sreenivasulu, M. Vetrichelvan, F. Zhao, S. Gao, J. J. Vittal, *Eur. J. Inorg. Chem.* **2005**, 4635 – 4645.
[17] J. M. Li, Y. L. Zhao, Y. M. Jiang, *Synth. React. Inorg. Met.-Org. Nano-Met. Chem.* **2010**, *40*, 715 – 718.
[18] Q. J Zhou, X. J Yao, L. F Hao, Y. Ouyang, J. Y Xu, C. Z Xie, J. S Lou, *Z. Anorg. Allg. Chem.* **2010**, *636*, 2487 – 2491.
[19] B. Sreenivasulu, F. Zhao, S. Gao, J. J. Vittal, *Eur. J. Inorg. Chem.* **2006**, 2656 – 2670.
[20] L. Casella, M. Gullotti, *J. Am. Chem. Soc.* **1981**, *103*, 6338 – 6347.
[21] L. Casella, M. Gullotti, *J. Am. Chem. Soc.* **1982**, *104*, 2386 – 2396.
[22] L. Casella, M. Gullotti, *Inorg. Chem.* **1986**, *25*, 1293 – 1303.
[23] Y. M. Jiang, S. H. Zhang, Q. Xu, Y. Xiao, *Acta Chim. Sin.* **2003**, *61*, 573 – 577.
[24] J. M. Li, K. H. He, Y. M. Jiang, *Z. Naturforsch.* **2012**, *67b*, 11 – 16.
[25] S. H. Zhang, Y. M. Jiang, K. B. Yu, *Acta Crystallogr.* **2005**, *E61*, m209–m211.
[26] S. H. Zhang, *J. Guilin Inst. Technology* **2004**, *24*, 391 – 393.
[27] L. Han, R. Wang, D. Yuan, B. Wu, B. Lou, M. Hong, *J. Mol. Struct.* **2005**, *737*, 55 – 59.
[28] B. D. Wagner, G. J. McManus, B. Moulton, M. J. Zaworotko, *Chem. Commun.* **2002**, 2176 – 2177.
[29] Y. J. Cui, Y. F. Yue, G. D. Qian, B. L. Chen, *Chem. Rev.* **2012**, *112*, 1126 – 1162.
[30] P. Angaridis, J. W. Kampf, V. L. Pecoraro, *Inorg. Chem.* **2005**, *44*, 3626 – 3635.
[31] Y. Y. Liu, G. S. Zhu, G. Z. Fan, S. L. Qiu, *Acta Crystallogr.* **2007**, *C63*, m159–m160.
[32] S. Muthu, Z. Ni, J. J. Vittal, *Inorg. Chim. Acta* **2005**, *358*, 595 – 605.
[33] R. Q. Fang, X. M. Zhang, *Inorg. Chem.* **2006**, *45*, 4801 – 4810.
[34] J. X. Li, Z. X. Du, J. Zhou, H. Q. An, S. R. Wang, B. Zhu, S. M. Zhang, S. H. Wu, W. P. Huang, *Inorg. Chim. Acta* **2009**, *362*, 4884 – 4890.
[35] G. M. Sheldrick, SHELXS-97, Program for the Solution of Crystal Structures, University of Göttingen, Göttingen (Germany) **1997**. See also: G. M. Sheldrick, *Acta Crystallogr.* **1990**, *A46*, 467 – 473.
[36] G. M. Sheldrick, SHELXL-97, Program for the refinement of Crystal Structures, University of Göttingen, Göttingen (Germany) **1997**. See also: G. M. Sheldrick, *Acta Crystallogr.* **2008**, *A64*, 112 – 122.